Modelling solute transport in soil columns using advective–dispersive equations with fractional spatial derivatives

F. San Jose Martinez , Y.A. Pachepsky , W.J. Rawls

Technical University of Madrid (UPM), Madrid, Spain
USDA-ARS, Beltsville, MD, USA

A B S T R A C T

Solute transport in soils is commonly simulated with the advective–dispersive equation, or ADE. It has been reported that this model cannot take into account several important features of solute movement through soil. Recently, a new model has been suggested that results in a solute transport equation with fractional spatial derivatives, or FADE. We have assembled a database on published solute transport experiments in soil columns to test the new model. The FADE appears to be a useful generalization of the ADE. The order of the fractional differentiation reflects differences in physical conditions of the solute transport in soil.

Keywords:
Fractional derivatives
Fractional advective–dispersive equation
Solute transport
Porous media
Soil columns experiments

1. Introduction

Advection and hydrodynamic dispersion are considered to be the dominant mechanisms of solute transport in the vadose zone, i.e. the variably saturated layer of soils and sediments between the soil surface and the aquifers [1]. The advection is associated with the average water flux or velocity. The hydrodynamic dispersion is conceptualised as a diffusion-like process and can be interpreted as the result of the Brownian motion of solute particles [2]. Under these assumptions, the parabolic advective–dispersive equation (ADE)

$$\frac{\partial c}{\partial t} = D\frac{\partial^2 c}{\partial x^2} - v\frac{\partial c}{\partial x} \tag{1}$$

is the mass conservation equation for the transport of inert (conservative) solute in homogeneous rigid porous media with stationary water flow. In Eq. (1), c is the solute concentration [$M\,L^{-3}$], D is the dispersion coefficient [$L^2\,T^{-1}$], v is the average pore water velocity [$L\,T^{-1}$], x is the distance [L], and t is the time [T]. The ADE has served as the theoretical framework to model the fate and transport of chemicals, and to address critical environmental issues stemming from agricultural practices or waste disposal operations in last decades [1].

The ADE fails to capture some important features of solute transport in soils [3–8]. On the one hand, the dispersion coefficient tends to increase with the distance of solute concentration observations. This is often mentioned as the scale effect on the dispersion process [9]. On the other hand, solute concentrations at the outlet of the soil columns approach expected asymptotic values slower than predicted by the ADE; the phenomenon is known as heavy tailing [10–12]. Such behaviour is sometime referred to as the anomalous or the non-Fickian dispersion.

The basic assumption of the ADE models for the transport of contaminants through soil is that the movements of solute particles are characterized by the Brownian motion [2]. The complexity of pore space in natural porous media makes the hypothesis of the Brownian motion far too restrictive in some cases. It has been suggested that, in the soil matrix, high velocity regions tend to be spatially continuous at all scales, and therefore a solute particle travelling faster than the mean is likely to do that over large distances. Similarly, slower particles are trapped in stagnant zones before they have a chance to move in the general direction of the flow. Invoking the notion of the Lévy motion can simulate this type of solute particle transport. The Lévy motion is a broader framework compared with the Brownian motion, and includes the persistence in movements of solute particles. Significant deviations from the mean are more likely to occur in Lévy motions than in the Brownian movement [13,14]. These features make Lévy motion an attractive generalization of Brownian motion when describing solute transport in porous media [9,15]. Brownian motion is a specific case of the Lévy motion.

Similarly to the ADE that can be derived assuming Brownian motion [2], solute transport equations can be derived for Lévy motions [16–22]. These equations include fractional derivatives. The

one-dimensional version of the fractional advective–dispersive equation (FADE) with symmetric dispersion is

$$\frac{\partial c}{\partial t} = -v\frac{\partial c}{\partial x} + \frac{1}{2}D_f\left(\frac{\partial^\alpha c}{\partial_+ x^\alpha} + \frac{\partial^\alpha c}{\partial_- x^\alpha}\right) \tag{2}$$

Here, D_f is the fractional dispersion coefficient [$L^\alpha T^{-1}$], the superscript α is the order of fractional differentiation, $1 < \alpha \leqslant 2$, c is the solute concentration [$M L^{-3}$], v is the flow velocity [$L T^{-1}$], x is the distance [L], and t is the time [T]. Fractional derivatives are integro-differential operators defined as [23]:

$$\frac{\partial^\alpha c}{\partial_+ x^\alpha}(x,t) = \frac{1}{\Gamma(m-\alpha)}\frac{\partial^m}{\partial x^m}\int_A^x (x-z)^{m-\alpha-1}c(z,t)dz \tag{3}$$

for the left-sided fractional derivative, and

$$\frac{\partial^\alpha c}{\partial_- x^\alpha}(x,t) = \frac{(-1)^m}{\Gamma(m-\alpha)}\frac{\partial^m}{\partial x^m}\int_x^B (z-x)^{m-\alpha-1}c(z,t)dz \tag{4}$$

for the right-sided fractional derivative. Here, m is the integer such that $m-1 < \alpha \leqslant m$, Γ is the gamma function and A and B are real numbers. Let us remark that in the case $\alpha = 2$ the FADE reduces to the ADE.

The FADE as a model to simulate solute transport in soils has been applied to data from both laboratory and filed-scale experiments [20,18,9,24–29]. Laboratory data are obtained from the so called miscible displacement experiments, in which the tracer solution infiltrates into originally tracer-free soil columns, and the dependence of the tracer concentration at the outlet on time, or breakthrough curve (BTC), is measured during the infiltration.

Most of the applications of the FADE to the solute transport to-date rely on analytical solutions of the initial value problem in the infinite domain. However, in many practical applications initial-boundary value problems in a finite domain need to be considered and numerical solutions are required. Several methods had been developed to solve the FADE numerically in the past few years [30–32,27,33,34,28,29].

The objective of this work was to compare the performances of both the classical model (ADE) and the fractional one (FADE) using a mass-conserving boundary condition and the numerical solution. We used published breakthrough data from miscible displacement experiments.

2. Numerical solution of FADE for soil columns

To derive a numerical scheme to solve FADE for finite length soil columns, we make use of Grünwald definitions of the left- and the right-sided fractional derivatives (3) and (4); for $1 < \alpha \leqslant 2$ they are, respectively,

$$\frac{\partial^\alpha c}{\partial_+ x^\alpha}(x,t) = \lim_{M_+\to\infty}\frac{1}{h_+^\alpha}\sum_{k=0}^{M_+} g_k\, c(x-kh,t) \tag{5}$$

and

$$\frac{\partial^\alpha c}{\partial_- x^\alpha}(x,t) = \lim_{M_-\to\infty}\frac{1}{h_-^\alpha}\sum_{k=0}^{M_-} g_k c(x+kh,t) \tag{6}$$

where $M_\pm$ are positive integers, $h_+ = x/M_+$, $h_- = (L-x)/M_-$, L is the length of the column. We have chosen $A = 0$ and $B = L$ in Eqs. (3) and (4), respectively. The Grünwald weights g_k are defined as

$$g_0 = 1, \quad g_k = (-1)^k\frac{\alpha(\alpha-1)\cdots(\alpha-k+1)}{k!} \tag{7}$$

In order to setup a numerical scheme let M be a nonnegative integer, h a real number such that $h = L/M$ and $x = ih$, $i = 0,1,\ldots,M$, for $0 \leqslant x_i \leqslant L$; also $t_n = n\Delta t$, so that $c_i^n = c(x_i,t_n)$. For the purpose of obtaining a stable numerical scheme, we used the shifted Grünwald approximation to the left-sided fractional derivatives (5) [33,34]

$$\frac{\partial^\alpha c}{\partial_+ x^\alpha}(x_i,t_n) \approx \frac{1}{h^\alpha}\sum_{k=0}^{M} g_k c(x_i-(k-1)h,t_n) \tag{8}$$

and the shifted Grünwald approximation to right-sided fractional derivatives (6)

$$\frac{\partial^\alpha c}{\partial_- x^\alpha}(x_i,t_n) \approx \frac{1}{h^\alpha}\sum_{k=0}^{M} g_k c(x_i+(k-1)h,t_n) \tag{9}$$

In these expressions g_k stand for the Grünwald weights (7). These approximations can be used in an explicit finite difference scheme for FADE

$$\frac{c_i^{n+1}-c_i^n}{\Delta t} = -v\frac{c_i^n - c_{i-1}^n}{h} + \frac{D_{sf}}{2h^\alpha}\left\{\sum_{k=0}^{M} g_k c_{i-k+1}^n + \sum_{k=0}^{M} g_k c_{i+k-1}^n\right\} \tag{10}$$

Note that for $\alpha = 2$, expressions (8) and (9) reduce to the standard centred difference formula for the second derivative and the explicit finite difference scheme (10) reduces to the standard explicit finite difference scheme for ADE. In the internal points of the spatial domain, ($i = 1,\ldots,M-1$), one has

$$c_i^{n+1} = B\sum_{k=0}^{i+1} g_k c_{i-k+1}^n + Ec_{i-1}^n + (1-E)c_i^n + B\sum_{k=0}^{M-i+1} g_k c_{i+k-1}^n + \Delta t s_i^n \tag{11}$$

Here $B = D\Delta t/2\,h^\alpha$ and $E = v\Delta t/h$. The stability condition is $v\Delta t/h + \alpha D\Delta t/h^\alpha \leqslant 1$.

Boundary conditions are needed to obtain the system of linear equations to find c_i^{n+1}, from c_i^n, $i = 1,\ldots,M-1$, in (11). When the analytical solutions of ADE are used with data from the miscible displacement experiments, the common approach is to use the solution for the semi-infinite domain, and to fit the simulated time series of the solute concentrations at the column outlet distance to the experimental BTC [35]. We followed this approach using numerical solutions by setting the zero concentration at the right boundary and moving it far enough, so that the concentration at this boundary at the end of the transport simulations would not be greater than 10^{-6} of the maximum inlet concentration.

At the inlet, the nodal concentrations were set to provide mass conservation [29]. If M_{ins}^n corresponds to the solute mass inside the column at the time step n and M_{ent} stands for the solute mass that has entered the transport domain at one time step, the conservation of the mass requires that

$$M_{ent} = M_{ins}^{n+1} - M_{ins}^n$$

This equation can be solved explicitly to obtain the boundary concentration c_0^{n+1}. The value of M_{ins}^n was computed as

$$M_{ins}^n = \sum_{i=1}^{M-1} c_i^n h + c_0^n(h/2)$$

When the tracer is injected into the soil column during the pulse time duration, t_p, one has $M_{ent} = v\Delta t$ for any timestep n such that $n\,\Delta t$ is smaller than t_p and $M_{ent} = 0$ otherwise. For a continuous pulse, t_p is infinite.

3. Data source and fitting procedure

We used published data on 53 breakthrough curves from seven experiment sets. Table 1 presents the information about experimental conditions. These experiments corresponded to miscible displacement in columns for a variety of soils (see Table 1) having different textures. The lengths and the diameters of the columns

Table 1
Selected experimental conditions, optimum values of parameter α and corresponding root-mean-squared errors (RMSE).

Soil	Disturbed/undisturbed	Tracer	Flow velocity (cm h^{-1})	Saturated	Water content	Optimum alpha	RMSE
Biggar and Nielsen [37]							
Columbia	Disturbed	Chloride	0.2	No	0.482	1.9	0.01104
Columbia	Disturbed	Tritium	0.2	No	0.482	2	0.01269
Columbia	Disturbed	Chloride	0.2	No	0.472	1.15	0.01736
Columbia	Disturbed	Tritium	0.2	No	0.472	1.55	0.01315
Cassel et al. [38]							
Beotia	Disturbed	Nitrate	0.0151	No	0.391	1.2	0.01262
Beotia	Disturbed	Chloride	0.0151	No	0.391	1.05	0.00261
Beotia	Undisturbed	Nitrate	0.0151	No	0.324	1.15	0.01085
Beotia	Undisturbed	Chloride	0.0151	No	0.324	1.45	0.00216
Aberdeen	Disturbed	Nitrate	0.0151	No	0.378	1.85	0.01005
Aberdeen	Disturbed	Chloride	0.0151	No	0.378	1.85	0.00515
Aberdeen	Undisturbed	Nitrate	0.0151	No	0.346	2	0.01888
Aberdeen	Undisturbed	Chloride	0.0151	No	0.346	1.95	0.01046
McMahon and Thomas [40]							
Maury	Undisturbed	Chloride	0.17	Yes	0.338	1.75	0.01884
Maury	Undisturbed	Tritium	0.17	Yes	0.338	1.15	0.02031
Maury	Disturbed	Chloride	0.17	Yes	0.339	2	0.02068
Maury	Disturbed	Tritium	0.17	Yes	0.339	1.55	0.0139
Pembroke	Undisturbed	Tritium	0.17	Yes	0.324	2	0.0122
Pembroke	Undisturbed	Chloride	0.17	Yes	0.324	1.75	0.01507
Pembroke	Disturbed	Tritium	0.17	Yes	0.335	1.65	0.01552
Pembroke	Disturbed	Chloride	0.17	Yes	0.335	2	0.02207
Eden	Undisturbed	Chloride	0.17	Yes	0.384	2	0.03931
Eden	Undisturbed	Tritium	0.17	Yes	0.384	1.6	0.01173
Eden	Disturbed	Chloride	0.17	Yes	0.396	1.3	0.01651
Eden	Disturbed	Tritium	0.17	Yes	0.396	1.05	0.01653
Rao et al. [39]							
Molokai	Disturbed	Tritium	5.82	Yes	0.626	1.7	0.00941
Wahiawa	Disturbed	Tritium	6.84	Yes	0.644	2	0.00778
Nielsen and Biggar [36]							
Yolo	Disturbed	Chloride	0.04	Yes	ND	2	0.01436
Yolo	Disturbed	Chloride	1.89	Yes	ND	1.2	0.0116
Columbia	Disturbed	Chloride	0.05	Yes	ND	2	0.0125
Columbia	Disturbed	Chloride	2.49	Yes	ND	2	0.00989
Oakley	Disturbed	Chloride	0.28	No	0.27	1.15	0.02465
Oakley	Disturbed	Chloride	0.27	No	0.33	1.15	0.03561
Oakley	Disturbed	Chloride	0.3	No	0.36	1.15	0.01176
Glass beads	Disturbed	Chloride	1.54	No	0.17	2	0.04636
Glass beads	Disturbed	Chloride	1.77	No	0.34	2	0.02578
Jardine et al. [42]							
ND	Undisturbed	Bromide	8.05	No	0.549	2	0.02635
ND	Undisturbed	Bromide	1.5	No	0.533	2	0.03431
ND	Undisturbed	Bromide	0.18	No	0.513	1.15	0.01006
ND	Undisturbed	Bromide	0.03	No	0.419	1.15	0.00548
Seyfried and Rao [41]							
Typic Distropept	Undisturbed	Tritium	26.4	Yes	0.57	2	0.03282
Typic Distropept	Undisturbed	Tritium	2.7	Yes	0.57	2	0.01075
Typic Distropept	Undisturbed	Tritium	19.5	Yes	0.57	2	0.02432
Typic Distropept	Undisturbed	Tritium	5.9	Yes	0.55	2	0.01022
Typic Distropept	Undisturbed	Tritium	1.2	No	0.53	2	0.01535
Typic Distropept	Undisturbed	Tritium	0.2	No	0.52	1.75	0.01052
Typic Distropept	Undisturbed	Tritium	28.7	Yes	0.6	2	0.0143
Typic Distropept	Undisturbed	Tritium	1.3	No	0.59	1.5	0.00661
Typic Distropept	Undisturbed	Tritium	19.7	Yes	0.55	2	0.06093
Typic Distropept	Undisturbed	Tritium	1.7	No	0.52	2	0.01258
Typic Distropept	Undisturbed	Tritium	29.4	Yes	0.54	2	0.07177
Typic Distropept	Undisturbed	Tritium	0.9	No	0.52	2	0.01747
Typic Distropept	Undisturbed	Tritium	24.7	Yes	0.53	2	0.01636
Typic Distropept	Undisturbed	Tritium	2.1	No	0.51	1.8	0.00649

varied between 10 and 84 cm and between 3.5 and 30 cm, respectively. Soil structure was natural in some columns, and was artificial, or disturbed, in others. Both water-saturated and unsaturated soils were used in the experiments. Chloride, tritium and bromide were the tracer ions. The flow velocities ranged between 0.015 and 29.4 cm h^{-1} (Table 1). The BTC data points were obtained by digitizing graphs found in the selected publications. The digitizing was made in triplicate. Coefficients of variation within the replications did not exceed 0.1%.

The range of α's ($1 < \alpha \leqslant 2$) was scanned in increments of 0.05. For each value of α, D_f and v were estimated using a version of the Marquardt–Levenberg algorithm [43] to minimize the root-mean-squared error (RMSE):

$$\mathrm{RMSE} = \sqrt{\sum_{j=1}^{N} \left(c_j^{calc} - c_j^{meas}\right)^2 / N} \tag{12}$$

where N is the number of observations.

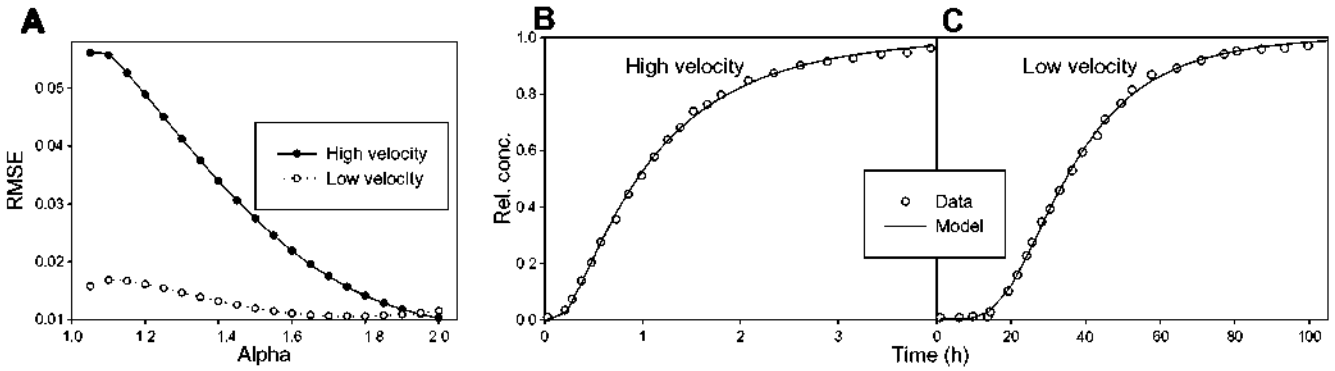

Fig. 1. Root-mean-squared error of the model fit and breakthrough curves. A – variation of RMSE with the order of the fractional derivative α of two Typic Distropept soils [41], filled circles with a flow velocity of 5.90 cm h^{-1} and hollow circles with a flow velocity of 0.20 cm h^{-1}; B and C – measured (symbols [41]) and simulated (solid lines) breakthrough curves of the high and low flow rates, respectively. The best fit was obtained for $\alpha = 2.0$ in the case of high flow rates and $\alpha = 1.75$ for the low flow case.

4. Results and discussion

Fig. 1 shows the typical result of the parameter estimation procedure. The dependence of the RMSE (12) values on the order of the fractional derivative α is shown in Fig. 1A for Typic Distropept soils with two different flow rates of 5.90 and 0.20 cm h^{-1}, and similar saturation degree of 0.550 and 520 water content, respectively [41]. The simulated BTC are compared with measured BTC in the plots 1B (high flow) and 1C (slow flow) for the values of α, D_f and v corresponding to the minimum RMSE. In both cases the minimum RSME were 0.010. In the case of high flow rates (Fig. 1B) this minimum value was attained with $\alpha = 2.0$ and with $\alpha = 1.75$ (Fig. 1C) in the case of low flow.

Overall, the FADE, as a general model that includes the ADE, accurately simulates experimental breakthrough curves from miscible experiments in soil columns. In this study, 31 out of 53 breakthrough curves are fitted with the RMSE less than 0.019 and the largest RSME is 0.072 (see Table 1).

From the 53 experimental BTCs considered, 28 are better fitted with α smaller than 2.00, i.e. with the FADE, and 25 are best fitted with $\alpha = 2.00$, i.e. with the classical ADE. This suggests the necessity to use the FADE rather than the ADE as a general framework to simulate solute transport in soil. The differences in values of the optimal parameter α presumably reflect different degrees of complexity of the solute particles movement in soil. The latter, in turn, might reflect the differences in the hierarchical structure of soil pore space for each particular case. Relating α to pore space geometry presents an interesting research avenue to explore. Data on soil pore space tomography coupled with the column transport data can be very useful in this respect.

Optimal values of α tended to vary with type of soil, type of tracer, flow velocity and saturation degree. For the Oakley soil from Ref. [36], α was 1.15 while it was 2.00 for the others soils of this dataset, except in the case of the Yolo soil with highest flow velocity (1.89 cm h^{-1}). In the dataset from Ref. [38] the optimal values of α for Beotia BTC's were lower than for Aberdeen soils; these values were between 1.05 and 1.45 for Beotia soils while α was between 1.85 and 2.00 for Aberdeen soils. There was also a substantial difference between Molokai and Wahiawa soils from Ref. [39]. In the case of the dataset from Ref. [40] the highest values of α corresponded to disturbed Maury and Pembroke soils under saturated conditions and chloride as a tracer.

Values of α were larger for tritium than for chloride. This was the case for the experiments in [37] under the same saturated conditions and also for the Maury (with high water content), Eden (with high water content) and Pembroke soils of the experiments in [40]. One reason for that may be the difference between pore spaces available to these two tracers. Chloride transport is affected by the anion exclusion that greatly decreases its concentrations in the vicinity of charged surfaces of soil particles.

The degree of soil saturation with water affected the optimum value of parameter α. In general, unsaturated soils had values of α smaller than two. This trend is particularly clear in the experiments from [38]. For the same soil, a decrease in the saturation degree produced a decrease in the optimum value of parameter α, e.g. data from [37,42]. The decrease in the saturation degree may create more complex pathways of the solute movement after emptying the large pores that dominate transport in saturated soil.

There was some interplay between effects of flow velocity and soil water saturation. The increase in the optimum value of α with the increase in flow velocity was observed with data from [36,39,42]. Lower values of α were related to lower flow velocities in the dataset from [41]. At the same saturation degree, one may expect the increase in pore water velocity to result in a more distinct separation of the pore space into slow- and high-speed transport zones, and therefore a larger probability for values of α to have values less than 2.

5. Conclusions

The FADE constitutes a broad framework that includes the ADE and considers solute particles undergoing motions that are more complex than Brownian motion. Differences in values of the parameter α presumably reflect differences in hierarchical geometries of soil pore spaces. The FADE has accurately simulated the breakthrough curves considered in this study. The values of α ranged from 1.05 to 2.00. From the 53 experimental breakthrough considered, 28 were better fitted with α smaller than two, and 25 are best fitted with ADE, i.e. $\alpha = 2$. Trends of the increase in values of α with the increase in saturation and in flow velocity have been observed for this particular dataset. The fractional advective–dispersive equation as a generalization of classical advective–dispersive equation is a promising enhancement in the hydrologist toolbox.

Acknowledgements

Fernando San José Martínez was supported in part by a grant of Secretaría de Estado de Universidades e Investigacion (Ministerio de Educacion y Ciencia, Spain), the Plan Nacional de Investigación Científica, Desarrollo e Innovación Tecnológica (I+D+I) under Ref. AGL2007-62648 Spain and DGUI (Comunidad de Madrid) and UPM (Universidad Politécnica de Madrid) under Ref. M 0700204135.

References

[1] Jury WA, Flühler H. Transport of chemical through soil: mechanics, models and flied experiments. Adv Agron 1992;47:141–201.

[2] Bhatacharya R, Gupta VK. Application of the central limit theorem to solute transport in saturated porous media: from kinetic to field scales. In: Cushman JH, editor. Dynamics of fluids in hierarchical porous media. New York: Academic Press; 1990. p. 97–124.

[3] Jury WA. Solute transport and dispersion. In: Steffen WL, Denmead OT, editors. Flow and transport in the natural environment: advances and applications. Berlin: Springer-Verlag; 1988. p. 1–16.

[4] Khan AUH, Jury WA. A laboratory test of the dispersion scale effect. J Contam Hydrol 1990;5:119–32.

[5] Porro I, Wierenga PJ, Hills RG. Solute transport through large uniform and layered soil columns. Water Resour Res 1993;29:1321–30.

[6] Snow VO, Clothier BE, Scotter DR, White RE. Solute transport in a layered field soil: experiments and modelling using the convection–dispersion approach. J Contam Hydrol 1994;16:339–58.

[7] Yasuda H, Berndtsson R, Barri A, Jinno K. Plot-scale solute transport in a semiarid agricultural soil. Soil Sci Soc Am J 1994;58:1052–60.

[8] Zhang R, Huang K, Xiang J. Solute movement through homogeneous and heterogeneous soil columns. Adv Water Resour 1994;17:317–24.

[9] Pachepsky YA, Benson DA, Rawls WJ. Simulating scale-dependent solute transport in soils with the fractional advective–dispersive equation. Soil Sci Soc Am J 2000;64:1234–43.

[10] van Genuchten MTh, Wierenga PJ. Mass transfer in sorbing porous media: I. Analytical solutions. Soil Sci Soc Am J 1976;40:473–81.

[11] Nielsen DR, van Genuchten MTh, Biggar JW. Water flow and solute transport processes in the unsaturated zone. Water Resour Res 1986;22(Suppl. 9):89S–108S.

[12] Vachaud G, Vauclin M, Addiscott TM. Solute transport in the vadose zone: a review of models. In: Proceedings of the international symposium on water quality modelling of agricultural non-point sources, Part 1, 19–23 June 1988, Logan, UT. USDA-ARS, US Gov. Print. Office, Washington, DC, 81–104; 1990.

[13] Bouchard JP. More Lévy distributions in physics. In: Shlesinger MF, Zaslavsky GM, Frisch U, editors. Lévy flights and related topics in physics. New York: Springer; 1995. p. 239–50.

[14] Weeks ER, Solomon TH, Urbach JS, Swinney HL. Observation of anomalous diffusion and Lévy flights. In: Shlesinger MF, Zaslavsky GM, Frisch U, editors. Lévy flights and related topics in physics. New York: Springer-Verlag; 1995. p. 51–71.

[15] Benson DA, Wheatcraft SW, Meerschaert MM. Application of a fractional advection–dispersion equation. Water Resour Res 2000;36(6):1403–12.

[16] Zaslavsky GM. Renormalization group theory of anomalous transport in systems with Hamiltonian chaos. Chaos 1994;4(1):25–33.

[17] Compte A. Stochastic foundations of fractional dynamics. Phys Rev E 1996;53(4):4191–3.

[18] Compte A. Continuous time random walks on moving fluids. Phys Rev E 1997;55(6):6821–31.

[19] Saichev AI, Zaslavsky GM. Fractional kinetic equations: solutions and applications. Chaos 1997;7:753–64.

[20] Benson DA. The fractional advection–dispersion equation: development and application. PhD thesis, University of Nevada, Reno; 1998.

[21] Chaves AS. A fractional diffusion equation to describe Lévy flights. Phys Lett A 1998;239:13–6.

[22] Metzler R, Klafter J, Sokolov IM. Anomalous transport in external fields: continuous time ransom walks and fractional diffusion equations extended. Phys Rev E 1998;58:1621–33.

[23] Samko SG, Kilbas AA, Marichev OI. Fractional integrals and derivatives: theory and applications. New York: Gordon and Breach Science Publ.; 1993.

[24] Benson DA, Schumer R, Meerschaert MM, Wheatcraft SW. Fractional dispersion, Levy motion, and the MADE tracer tests. Transp Porous Media 2001;42:211–40.

[25] Lu S, Molz FJ, Fix GJ. Possible problems of scale dependency in applications of the three-dimensional fractional advection–dispersion equation to natural porous media. Water Resour Res 2002;38(9):1165. doi:10.1029/2001WR000624.

[26] Zhou LZ, Selim HM. Application of the fractional advection–dispersion equation in porous media. Soil Sci Soc Am J 2003;67(4):1079–84.

[27] Deng ZQ, Singh VP, Bengtsson L. Numerical solution of fractional advection–dispersion equation. ASCE J Hydraul Eng 2004;130(5):422–31.

[28] Zhang X, Crawford JW, Deeks LK, Stutter MI, Bengough AG, Young IM. A mass balance based numerical method for the fractional advection–dispersion equation: theory and application. Water Resour Res 2005;41:W07029. doi:10.1029/2004WR003818.

[29] San Jose Martinez F, Pachepsky YA, Rawls W. Solute transport simulated with the fractional advective–dispersive equation. In: Agrawal O, Tenreiro Machado JA, Sabatier J, editors. Fractional derivatives and their applications, IDECT/CIE2005; 2005. ISBN: 0-7918-3766-1.

[30] Lynch VE, Carreras BA, del-Castillo-Negrete D, Ferreiras-Mejias KM, Hicks HR. Numerical method for the solution of partial differential equations with fractional order. J Comput Phys 2003;192:406–21.

[31] Oldham KB, Spanier J. The fractional calculus. New York: Academic Press; 1974.

[32] Liu F, Anh V, Turner I. Numerical solution of the space fractional Fokker–Planck equation. J Comput Appl Math 2004;166:209–19.

[33] Meerschaert MM, Tadjeran C. Finite difference approximation for fractional advection–dispersion flow equations. J Comput Appl Math 2004; 172:65–77.

[34] Meerschaert MM, Tadjeran C. Finite difference approximations for two-sided space-fractional partial differential equations. Appl Numer Math 2006; 56:80–90.

[35] Toride N, Leij FJ, van Genuchten MTh. The CXTFIT code for estimating transport parameters from laboratory or field tracer experiments. Version 2.0. Research rep 137, US Salinity Lab, Riverside (CA); 1995.

[36] Nielsen DR, Biggar JW. Miscible displacement in soils: I. Experimental information. Soil Sci Soc Proc 1961;25:1–4.

[37] Biggar JW, Nielsen DR. Miscible displacement in soils: II. Behaviour of tracers. Soil Sci Soc Proc 1962;26:125–8.

[38] Cassel DK, Krueger TH, Schroer FW, Norum EB. Solute movement through disturbed and undisturbed soil cores. Soil Sci Soc Am Proc 1974;38:36–40.

[39] Rao PSC, Green RE, Ahuja LR, Davidson JM. Evaluation of a capillary bundle model for describing solute dispersion in aggregated soils. Soil Sci Soc Am J 1976;40:815–20.

[40] McMahon MA, Thomas GW. Chloride and titrated water flow in disturbed and undisturbed soil cores. Soil Sci Soc Am Proc 1974;28:727–32.

[41] Seyfried MS, Rao PSC. Solute transport in undisturbed columns of an aggregated tropical soil: preferential flow effect. Soil Sci Soc Am J 1987;51: 1434–44.

[42] Jardine PM, Jacobs GK, Wilson GV. Unsaturated transport processes in undisturbed heterogeneous porous media: I. Inorganic contaminants. Soil Sci Soc Am J 1993;57:945–53.

[43] van Genuchten MTh. Non-equilibrium transport parameters from miscible displacement experiments. Research Rep. No. 119, US Salinity Laboratory, USDA-SEA-ARS, Riverside (CA); 1981.